

- [16] The chiral environment was obtained by the addition of an appropriate amount of enantiopure (*R*)-(-)-1-(9-anthryl)-2,2,2-trifluoroethanol to a CDCl₃ solution (see: W. H. Pirkle, *J. Am. Chem. Soc.* **1966**, *88*, 1837).
- [17] Under conditions of fast exchange, two averaged lines should actually be observable, one for each pair of *ortho* carbon atoms of the two rapidly rotating phenyl groups. However, the separation of these two averaged lines ($\Delta\delta = 0.6$) is too small to be resolved, as also shown by the computer line-shape simulation (see Figure 3).
- [18] F. G. Riddell, S. Arumagam, J. E. Anderson, *J. Chem. Soc. Chem. Commun.* **1991**, 1525; P. J. Barrie, J. E. Anderson, *J. Chem. Soc. Perkin Trans. 2* **1992**, 2031; F. G. Riddell, S. Arumagam, K. D. M. Harris, M. Rogerson, J. H. Strange, *J. Am. Chem. Soc.* **1993**, *115*, 1881; A. E. Aliev, K. D. M. Harris, D. C. Apperley, *J. Chem. Soc. Chem. Commun.* **1993**, 251; F. G. Riddell, G. Bernath, F. Fülöp, *J. Am. Chem. Soc.* **1995**, *117*, 2327; D. Casarini, L. Lunazzi, A. Mazzanti, *J. Org. Chem.* **1998**, *63*, 9125; L. Lunazzi, A. Mazzanti, D. Casarini, O. De Lucchi, F. Fabris, *J. Org. Chem.* **2000**, *65*, 883; J. E. Anderson, D. Casarini, L. Lunazzi, A. Mazzanti, *J. Org. Chem.* **2000**, *65*, 1729; D. Casarini, L. Lunazzi, A. Mazzanti, G. Simon, *J. Org. Chem.* **2000**, *65*, 3207.
- [19] This feature guarantees that the observed dynamic process cannot be caused by a 180° rotation of the whole molecule within the crystal, leading to an exchange of the positions of the two phenyl groups. In this case, the signals of the quaternary and *para* carbon atoms should also have displayed line-broadening effects, as observed with the signals for the *ortho* carbon atoms.
- [20] Use was made of a PC version of the DNMR6 computer program n° 633 of QCPE, Indiana University, Bloomington, IN, USA.
- [21] The shift separation between the inner pair of lines ($\Delta\delta = 3.9$) is too close to that between the outer pair ($\Delta\delta = 5.5$)^[8] to account for the observed line shape on the basis of a unique free energy of activation, as clearly demonstrated by the computer simulation. When the two rings were assumed to have identical rotation rates (i.e. coincident ΔG^\ddagger values), it was impossible to reproduce the experimental dynamic spectra of Figure 3.
- [22] As is usually observed in rotation processes, in the present experiment the ΔG^\ddagger values were found also to be independent of temperature, which indicates a negligible value for the corresponding ΔS^\ddagger ; see: D. Casarini, L. Lunazzi, E. Foresti, D. Macciantelli, *J. Org. Chem.* **1994**, *59*, 4637.
- [23] An example of this type is provided by the two different rotation barriers measured for the *tert*-butyl substituents in (*t*Bu)₂CH(*i*Pr), owing to the molecule adopting a chiral conformation when the CH-*i*Pr bond rotation is frozen (J. E. Anderson, B. R. Bettels, H. M. R. Hoffman, P. Pauluth, S. Hellmann, H. D. Beckhaus, C. Ruchardt, *Tetrahedron* **1988**, *44*, 3701).
- [24] F. W. Wehrli, A. P. Marchand, S. Wherli, *Interpretation of C-13 NMR Spectra*, 2nd ed., Wiley, Chichester, **1988**, pp. 74–75.
- [25] D. Casarini, L. Lunazzi, A. Mazzanti, *J. Org. Chem.* **1998**, *63*, 9125; see also: A. E. Aliev, K. D. M. Harris, *Magn. Reson. Chem.* **1994**, *32*, 366.

Exceptionally Long (≥ 2.9 Å) C–C Bonds between [TCNE][−] Ions: Two-Electron, Four-Center $\pi^*-\pi^*$ C–C Bonding in π -[TCNE]₂^{2−}

Juan J. Novoa,* Pilar Lafuente, Rico E. Del Sesto, and Joel S. Miller*

Dedicated to the memory of Linus Pauling on the occasion of the 100th anniversary of his birth

We present here an exceptionally long C–C bonding interaction that has spectroscopic (IR and UV/Vis), structural, and magnetic properties expected for a bond and that complies with Pauling's definition of a chemical bond.^[1] Strong carbon–carbon bonding is the essence of organic chemistry. The length of a C–C single bond, that is, 1.54 Å found in the diamond allotrope of carbon, is among the essential information learned by all organic chemistry students. This is the length of a single bond between sp³-hybridized carbon atoms and is the longest of all common C–C bonds, although elongated C–C bonds as long as 1.73 Å have been reported.^[2] These bonds form whenever two carbon atoms possessing an unpaired electron are close to each other (e.g., as occurs for two ·CH₃ radicals, which form ethane). When the carbon atoms are radical anions (or radical cations), due to their strong coulombic repulsion, bonds do not form. Thus, many electron transfer salts involving radicals are stable, and as a consequence exhibit interesting electrical and optical properties. Herein, however, we show that C–C interactions having all the properties of a chemical bond are present between pairs of [TCNE][−] ions in some TCNE-based electron transfer salts, and that this type of bonding is present for many other reduced strong electron acceptors, for example, cyanil,^[3] 7,7,8,8-tetracyano-*p*-quinodimethane (TCNQ),^[4] perfluoro-7,7,8,8-tetracyano-*p*-quinodimethane (TCNQF₄),^[5] and 2,3-dichloro-5,6-dicyanobenzoquinone (DDQ).^[6]

Strong organic electron acceptors (**A**) such as TCNE and TCNQ form stable electron transfer salts that contain [**A**][−]. These salts were crucial for the discovery and development of molecule-based metals,^[7] which subsequently led to the discovery of molecule-based superconductors,^[8] as well as molecule-based magnets.^[9]

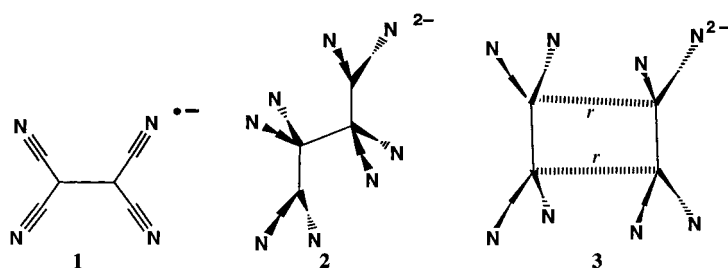
[*] Prof. J. J. Novoa, P. Lafuente
Department of Physical Chemistry
University of Barcelona
Av. Diagonal, 647, 08028 Barcelona (Spain)
Fax: (+34) 93-402-1231
Prof. J. S. Miller, R. E. Del Sesto
Department of Chemistry
University of Utah
Salt Lake City, UT, 84112 (USA)
Fax: (+1) 801-581-8433

[**] The authors gratefully acknowledge the support from the U.S. National Science Foundation (Grant No. CHE9320478) and the U.S. DOE (Grant No. DE FG 03-93ER45504). J.J.N. and P.L. also thank for support by CICYT (project PB98-1166-C02-02) and CIRIT (1999SGR-00046), and a grant of computer time provided by CESCA-CEPBA and the University of Barcelona. In addition, P.L. thanks the Ministerio de Educación y Cultura for her doctoral fellowship grant.



Supporting information for this article is available on the WWW under <http://www.angewandte.com> or from the author.

Open-shell $[A]^{\cdot-}$ species can form numerous structures; examples are $[TCNE]^{\cdot-}$ (1),^[10] its σ dimer octacyanobutane-1,4-diide, $[C_4(CN)_8]^{2-}$ (2),^[11] and its π dimer, $[TCNE]_2^{2-}$ (3).^[12–19] $[M^{II}(NCMe)_2[C_4(CN)_8]]$ ($M = Mn, Fe$) are examples of 2 and



possess the octacyanobutane-1,4-diide dianion $\mu_4-[C_4(CN)_8]^{2-}$ ^[11, 20] with a long (1.6 Å) central $C_{sp^3}-C_{sp^3}$ σ bond.^[11] Structure 3, as well as other $\pi-[A]_2^{2-}$ dimers, represents an unusual class of organic compounds as they possess exceptionally long (≥ 2.83 Å) π -bonding interactions,^[18] which are substantially less than the π -C van der Waals radius of 3.4 Å, and the cyano substituents deviate by 3.6 to 6.5° (one-half of the *trans*-NC...CN dihedral angle) from the formal TCNE plane. These are π dimers because the intradimer C–C bonding primarily occurs through overlap of the π^* orbitals at the four central sp^2 -like carbon atoms. The presence of bonding is experimentally supported by structural, spectroscopic (UV/Vis and IR), and magnetic data (vide infra).

These dimers self-assemble to form supramolecular aggregates. The intradimer $\pi^*-\pi^*$ C–C distances are twice that of a typical C–C bond and have properties that differ from those of van der Waals interactions, but are similar to those associated with normal covalent bonds. Hence, to understand the unusual nature of the long C–C bonding, the electronic structure, IR spectra, diamagnetic behavior, and stability of these $\pi-[A]_2^{2-}$ dimers, we embarked upon a systematic computational and experimental study of $\pi-[TCNE]_2^{2-}$ dimers.^[21, 22]

The properties of the $[TCNE]_2^{2-}$ dimers (Table 1) arise from the unpaired electron on each of the monomers and their anionic character. Consequently, two factors dominate the formation of these dimers: 1) the electrostatic repulsion (E_{coul}) between two anionic $[TCNE]^{\cdot-}$ fragments, and 2) the

attractive forces arising from intradimer bonding (E_{bond}), either σ or π , that is, $E_{int} = E_{coul} + E_{bond}$. The energy E_{coul} for the anion–anion interaction is always repulsive, while E_{bond} is taken as being attractive, as it corresponds to the interaction of two singly occupied molecular orbitals (SOMOs). When $E_{coul} > E_{bond}$, the $[A]^{\cdot-}$ units repel each other and there is no minimum-energy structure. If $E_{bond} > E_{coul}$ there will be a stable energy minimum on the potential energy surface (Figure 1). Additionally, when $E_{bond} \sim E_{coul}$ metastable dimers

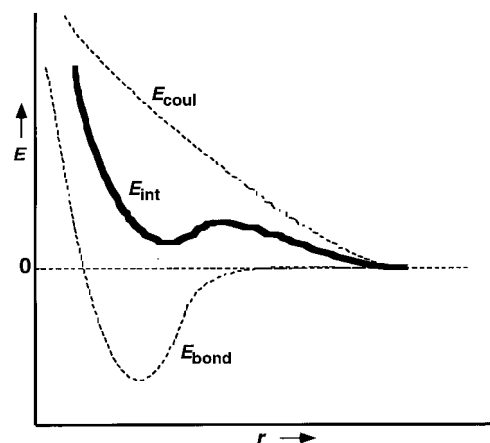


Figure 1. The total interaction energy curve (E_{int}) and its coulombic (E_{coul}) and bonding (E_{bond}) components.

form, that is, the energy of such a minimum lies above the energy of two $[A]^{\cdot-}$ monomers, but the dimer does not break into these fragments due to the presence of a barrier towards dissociation (Figure 1). Although metastable species cannot form in the gas phase at finite temperature, it can occur in a crystal if 1) the thermal energy is smaller than the barrier for the formation of the dimer from the fragments, or 2) the attractive electrostatic interactions with the cations are sufficient to overcome the coulombic energy barrier of $[TCNE]_2^{2-}$. Otherwise the dimers are repulsive. The existence of $[TCNE]_2^{2-}$ dimers in the solid state^[11, 12] is consistent with either a stable or a metastable dimer being formed, although the latter is the situation (vide infra).

The stability of the isolated $\pi-[TCNE]_2^{2-}$ dimer can be estimated by computing the shape of the $[TCNE]^{\cdot-} \cdots [TCNE]^{\cdot-}$ gas-phase potential energy surface as a function of the intradimer separation r .^[23] The RB3LYP

Table 1. Intradimer C–C distances, deviation from planarity, vibrational frequencies for structurally characterized $\pi-[TCNE]_2^{2-}$ dimers (s, m, and w indicate a strong, medium, or weak band, respectively).

Compound	Form	Intradimer C–C distance [Å]	C–C distance [Å]	Deviation from plane ^[a] [deg]	ν_{CN} [cm^{-1}]
$[Cu(PPh_3)(TCNE)]_2$ ^[12]	$\pi-[TCNE]_2^{2-}$	2.92	1.397	5.1	2193 w, 2173 m, 2162 s
$[Cr(C_6H_5)_2][TCNE]_2$ ^[13]	$\pi-[TCNE]_2^{2-}$	2.904	1.436	6.0	2189 m, 2170 s, 2159 s
$[Cr(C_6Me_5H_2)_2][TCNE]_2$ ^[13]	$\pi-[TCNE]_2^{2-}$	3.09	1.45	5.2	[b]
$[Fe(C_3H_4)_2C_3H_6][TCNE]_2$ ^[14, 16]	$\pi-[TCNE]_2^{2-}$	2.90	1.35	5.5	2191 m, 2169 s, 2161 s
$[K(glyme)]_2[TCNE]_2$ ^[15]	$\pi-[TCNE]_2^{2-}$	2.987	1.423	3.6	[b]
$[Fe(C_3H_5)(C_3Me_5)]_2[TCNE]_2(THF)$ ^[16]	$\pi-[TCNE]_2^{2-}$	2.90	1.372	5.75	2190 m, 2173 s, 2159 s
$[Fe(C_3H_5)(C_3Me_5)]_2[TCNE]_2(CH_2Cl_2)$ ^[16]	$\pi-[TCNE]_2^{2-}$	2.833	1.441	6.45	2190 m, 2173 s, 2160 s
$[(Me_2N)_2CC(NMe_2)_2][TCNE]_2$ ^[18, 19]	$\pi-[TCNE]_2^{2-}$	2.922	1.406	4.0	2193 m, 2174 s, 2163 s
$Tl_2[TCNE]_2$ ^[18]	$\mu_4-\pi-[TCNE]_2^{2-}$	2.874	1.51	4.5	2190 s, 2173 sh, 2162 s

[a] Calculated from one-half of the average *trans*-NC...CN dihedral angle using CrystalMaker4. [b] Not reported.

curve (Figure 2) indicates that the $[\text{TCNE}]^{\cdot-} \cdots [\text{TCNE}]^{\cdot-}$ interaction is repulsive and has two metastable minima, located at short (ca. 1.8 Å) and long distance (ca. 3.1 Å), which when fully optimized were found to be minimum-energy structures.^[24, 25] Their optimal geometry is close to the observed structures (see Supporting Information). However,

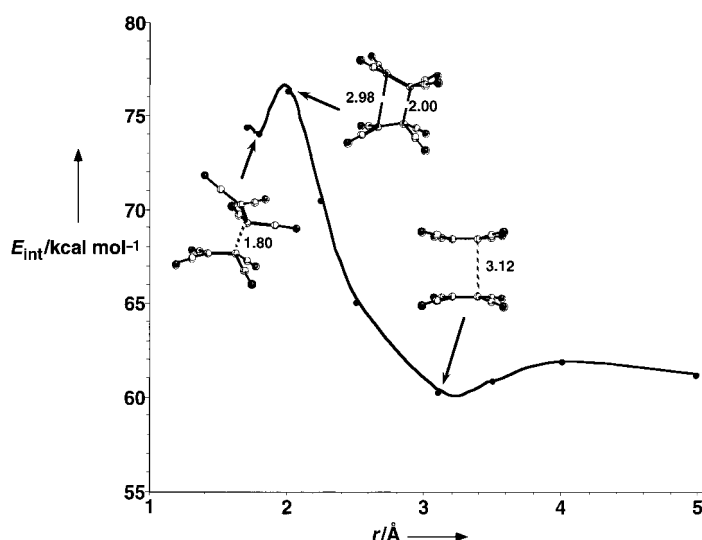


Figure 2. Computed adiabatic potential energy surface along r for the π - $[\text{TCNE}]_2^{2-}$ dimer at the RB3LYP level.

UB3LYP and MCSCF calculations using the same basis set indicated that there are no long-distance minima, that is, that the minima found at the RB3LYP level are a result of the double occupancy restriction imposed on the wavefunctions. As this double occupancy is not physically necessary, the dimers possess no real minima at long distances. The absence of a minimum is attributed to the electrostatic component (E_{coul}) between the anions, which exceeds the E_{bond} component. Therefore, the dimers in the crystalline state are a consequence of the attractive cation $\cdots [\text{TCNE}]^-$ interaction that exceeds the repulsive $[\text{TCNE}]^- \cdots [\text{TCNE}]^-$ interaction and gives rise to energetically stable neutral (cation) $_n[\text{TCNE}]_m$ supramolecular aggregates, for example, $n = m = 2$.^[26]

This is computationally illustrated for $[\text{K}(\text{glyme})]_2[\text{TCNE}]_2$ ^[15, 27] (Figure 3). The energetic stability of the π - $[\text{TCNE}]_2^{2-}$ dimer is attributed to $\text{K}_2[\text{TCNE}]_2$, which possesses a π - $[\text{TCNE}]_2^{2-}$ dimer and two K^+ ions (2.91 ± 0.16) Å from the N atoms nominally midway between the two parallel $[\text{TCNE}]^-$ planes (Figure 3). The intradimer C–C separation is about 3.0 Å, which is significantly less than the sum of the van der Waals radii of 3.4 Å; the C–C interdimer separation is about 4.5 Å. At the UHF/6-31 + G(2d,2p) level the $[\text{TCNE}]_2^{2-}$ with the short intradimer distance has a repulsive interaction of 103.0 kcal mol⁻¹ in its lowest triplet state. However, the $\text{K}^+ \cdots [\text{TCNE}]^-$ interactions within the $\text{K}_2[\text{TCNE}]_2$ fragment are attractive by 75.0 kcal mol⁻¹. Thus, although the $[\text{TCNE}]_2^{2-}$ dimers are energetically unstable with respect to dissociation, neutral $\text{K}_2[\text{TCNE}]_2$ is stable with respect to dissociation by 158.4 kcal mol⁻¹.^[28] This is typical of the interactions found in many ionic molecular crystals, whose energetics can be studied by ab initio methods and the proper

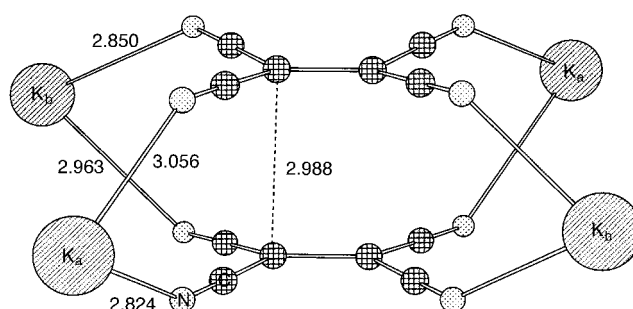


Figure 3. Geometry of the neutral $\text{K}_2[\text{TCNE}]_2$ unit used to calculate the energetics of the intermolecular interaction in the $[\text{K}(\text{glyme})]_2[\text{TCNE}]_2$ crystal.^[15] The key intermolecular distances between the fragments are given in Å. Note that there are two different crystallographic K^+ sites and thus two combinations for the $\text{K}_2[\text{TCNE}]_2$ aggregate. In our calculations each combination was used independently and the results were averaged. The unit has a net charge of zero.

model units.^[29] Therefore, despite the repulsive nature of the interaction between the two $[\text{TCNE}]^{\cdot-}$ ions of the $\text{K}_2[\text{TCNE}]_2$ supramolecular fragment, these anions form a dimer with a short intradimer separation of 3 Å. As a consequence, the singly occupied π^* orbitals of the $[\text{TCNE}]^{\cdot-}$ monomers overlap, leading to intermolecular bonding and antibonding dimer orbitals separated by a nonnegligible energy gap, Δ , that is similar to the one observed for energetically stable bonds. Due to this gap, the $[\text{TCNE}]_2^{2-}$ intradimer interactions exhibit all the structural, spectroscopic, and magnetic properties of a bond, as discussed below.

Ab initio UBLYP/6-31 + G(2d,2p) calculations^[30] on an isolated $[\text{TCNE}]^{\cdot-}$ fragment show that it has a planar structure similar to that of TCNE^0 ^[31] obtained with the same geometry and method, except that the central C–C distance increases from 1.367 Å in TCNE^0 to 1.437 Å in the $[\text{TCNE}]^{\cdot-}$, while the C≡N distance undergoes a minor increase from 1.158 to 1.167 Å. The extra electron resides in the b_{2g} SOMO of π^* symmetry (Figure 4), which is primarily located in the central C–C bond and on the N atoms, with similar weights for those C and N atoms. Likewise, the Mulliken population analysis indicates that the extra electron is equally shared by these C and N atoms (ca. 0.18 e^- per atom), in agreement with

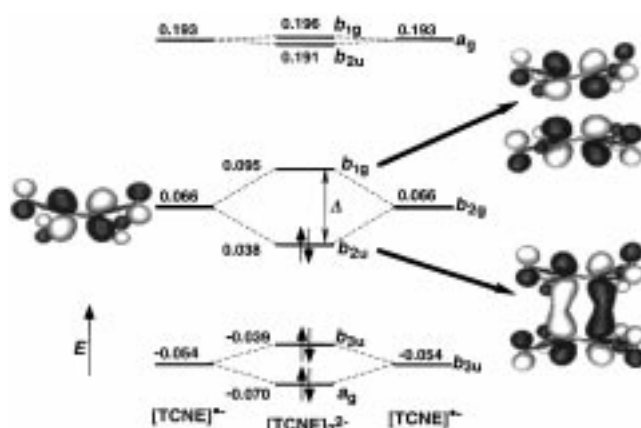


Figure 4. Shape of the π - $[\text{TCNE}]_2^{2-}$ dimer orbitals generated from the SOMO orbital of the $[\text{TCNE}]^{\cdot-}$ fragments.

the experimental data.^[32–34] Similar results were obtained by using UHF and MCSCF methods.

When the b_{2g} SOMOs of two $[\text{TCNE}]^{\cdot-}$ fragments overlap in the π - $[\text{TCNE}]_2^{2-}$ dimer, bonding and antibonding orbitals of b_{2u} and b_{1g} symmetry, respectively, form (Figure 4). When the energy separation between these two orbitals, $\Delta(r)$ (Figure 4), is small, which occurs at large values of r , as those found in the $\pi^*-\pi^*$ C–C bonds, each orbital will be singly occupied and $b_{2u}^1b_{1g}^1$ is the most stable configuration.

The presence of $\Delta(r)$ greater than zero gives rise to two singlet states, namely 1^1A_{1g} and 2^1A_{1g} , whose energy difference is the source of a UV/Vis electronic transition, and a new absorption is observed at about $15\,300\text{ cm}^{-1}$ (654 nm , 1.90 eV) for $\text{Ti}_2[\text{TCNE}]_2$ ($r=2.874\text{ \AA}$)^[19] (Figure 5a), $[(\text{Me}_2\text{N})_2\text{CC}(\text{NMe}_2)_2][\text{TCNE}]_2$ ($r=2.922\text{ \AA}$)^[18] and $[\text{Cr}^1(\text{C}_6\text{H}_6)]_2[\text{TCNE}]_2$ ($r=2.904\text{ \AA}$)^[13]. This absorption also explains the observed dark blue-purple color of these dimeric compounds. The disagreement between the experimental and calculated values is expected due to the approximate nature of the CIS method,^[35] in particular, to the limitations that the method presents for the accurate description of excited states. Another possible source of error is the use of isolated π - $[\text{TCNE}]_2^{2-}$ dimers in the calculations, as such a model cannot properly account for variations induced by the cations in the electronic structure of the dimers.

It is also a manifestation of bond formation that the IR spectrum of the dimer differs from that of its fragments. $[\text{TCNE}]^{\cdot-}$ has two strong^[36] $\nu_{\text{C}\equiv\text{N}}$ vibrations at around 2200 cm^{-1} (calcd), which correspond to the experimentally observed absorptions at 2183 and 2144 cm^{-1} .^[31b] In contrast, for π - $[\text{TCNE}]_2^{2-}$ three $\nu_{\text{C}\equiv\text{N}}$ vibrations are obtained at the RB3LYP/6-31+G level indicative of bond formation between the two $[\text{TCNE}]^{\cdot-}$ fragments. This is in accord with the average observed $\nu_{\text{C}\equiv\text{N}}$ absorptions at 2191 m , 2172 s , and 2161 s cm^{-1} (Table 1). Furthermore, a characteristic high-intensity absorption at about 1400 cm^{-1} , not observed for $[\text{TCNE}]^{\cdot-}$, is predicted for the π - $[\text{TCNE}]_2^{2-}$ dimer. This new absorption is due to the antisymmetric combination of the intrafragment C–C stretches of each fragment's central C–C bond, which becomes allowed and gains intensity due to electron-vibrational coupling.^[37] This absorption, which has been experimentally elusive as it is obscured by the Nujol matrix, occurs at 1361 cm^{-1} in a KBr matrix for both $\text{Ti}_2[\text{TCNE}]_2$ ^[18] (Figure 5b) and $[\text{Cr}^1(\text{C}_6\text{H}_6)]_2[\text{TCNE}]_2$.^[13] Thus, the π - $[\text{TCNE}]_2^{2-}$ dimer can be experimentally identified by 1) an additional strong $\nu_{\text{C}\equiv\text{N}}$ absorbance, 2) the shift of the three $\nu_{\text{C}\equiv\text{N}}$ absorbances towards higher frequencies, and 3) a new absorption at around 1360 cm^{-1} .

Another manifestation of the intradimer C–C bonding is the change in hybridization of the central carbon atoms as the intradimer distance decreases. This decrease is followed by changes in the *trans*-NC–C–C–CN angle, while the CN substituents move out of the $[\text{TCNE}]^{\cdot-}$ plane by 3.6 – 6.5° (av 5.1°), Table 1. This change is also observed in the optimized geometries in Figure 2, and is the expected when a C–C bond is formed with an sp^2 C atom. Intradimer bond formation also affects the magnetic properties. When doublet $[\text{TCNE}]^{\cdot-}$ fragments approach each other to form the π - $[\text{TCNE}]_2^{2-}$ dimer, $\Delta(r)$ and the singlet–triplet separation increase, such

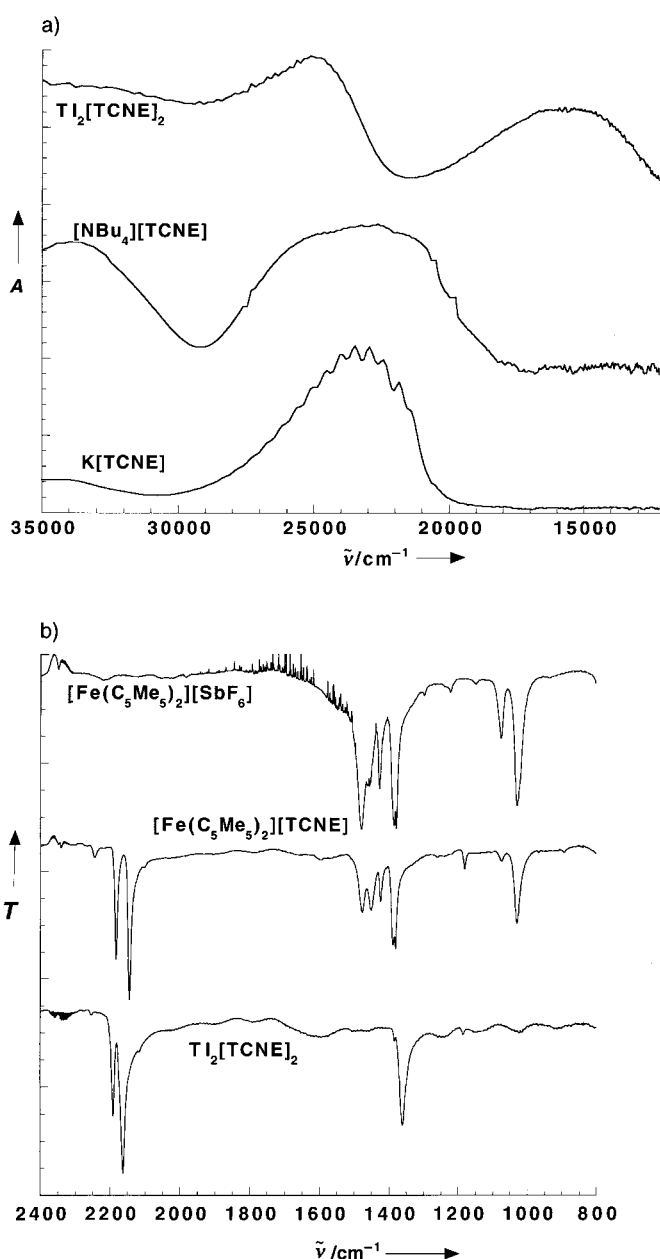


Figure 5. Experimental UV/Vis (a) and IR spectra (b) of some $[\text{TCNE}]^{\cdot-}$ salts. The absorption at $25\,000\text{ cm}^{-1}$ for solid $\text{Ti}_2[\text{TCNE}]_2$ (KBr pellet) is assigned to a transition in $[\text{TCNE}]^{\cdot-}$ similar to the one observed for $\text{K}[\text{TCNE}]$ in solution (30 mm in MeCN). The UV/Vis spectrum of $[\text{NBu}_4][\text{TCNE}]$ was recorded as a KBr pellet. In addition to the IR spectrum of $[\text{TCNE}]^{\cdot-}$ as the $[\text{Fe}(\text{C}_5\text{Me}_5)_2]^+$ salt, the spectrum of a $[\text{Fe}(\text{C}_5\text{Me}_5)_2]^+$ salt whose anion does not absorb in this region is given to help elucidating the contribution of the cation to the spectrum of $[\text{Fe}(\text{C}_5\text{Me}_5)_2][\text{TCNE}]$.

that the antiferromagnetically coupled singlet state is the only state that is thermally populated.

The observed properties of the π - $[\text{TCNE}]_2^{2-}$ dimer are consistent with those expected from the formation of a covalent C–C bond between two $[\text{TCNE}]^{\cdot-}$ ions. However, due to the repulsive electrostatic interactions, the $[\text{TCNE}]^{\cdot-} \cdots [\text{TCNE}]^{\cdot-}$ interactions are energetically unstable unless stabilized by the presence of cations. In contrast, the neutral system (cation) $_2[\text{TCNE}]_2$ is energetically stable due to the

attractive electrostatic cation...[TCNE][−] interactions, and enables the direct overlap of the SOMOs of the [TCNE][−] monomers through four carbon atoms and thus is responsible for the existence of cation-mediated $\pi^*-\pi^*$ C–C covalent bonding that occurs in the (cation)₂[TCNE]₂ aggregates. As this two-electron bond emerges from the overlap of the SOMO orbitals of the [TCNE][−], it is not hypervalent.^[38] Therefore, it cannot be present when the HOMO is doubly occupied. Hence, this cation-mediated $\pi^*-\pi^*$ C–C bond complies with Pauling's definition of a chemical bond,^[1] a key tenet of chemistry, and exhibits all the physical properties expected from a classical C–C covalent bond.

In summary, the formation of π -[TCNE]₂^{2−} dimers from the corresponding monomers is endothermic, due to repulsive electrostatic anion...anion interactions, but they can be stabilized by energetically stronger attractive electrostatic anion...cation interactions. When the [TCNE][−]...[TCNE][−] distance is sufficiently short, cation-mediated sub-van der Waals $\pi^*-\pi^*$ C–C bonding between the [TCNE][−] ions' central C–C bonds occurs by self-assembly. This supramolecular (K⁺)₂[TCNE]₂^{2−} aggregate is stable by 158.4 kcal mol^{−1}, and the two-electron, four-center $\pi^*-\pi^*$ C–C bonding leads to structural, spectroscopic, and magnetic consequences that are observed. Structurally, in addition to the $\pi^*-\pi^*$ C–C bonds with sub-van der Waals distances of about 2.9 Å, the CN substituents deviate from the [TCNE][−] plane by 3.6 to 6.5°. Spectroscopically, a new IR absorption occurs at around 1360 cm^{−1} ($\nu_{\text{C}=\text{C}}$), the two $\nu_{\text{C}=\text{N}}$ absorptions observed for isolated [TCNE][−] shift to higher energy, and a third $\nu_{\text{C}=\text{N}}$ absorption appears; the characteristic $\nu_{\text{C}=\text{N}}$ values are 2191 m, 2172 s, and 2161 s cm^{−1}. Also, a new electronic absorption assigned to the S₀→S₁ ($b_{2u}^2b_{1g}^0$; $^1A_{1g} \rightarrow b_{2u}^1b_{1g}^1$; $^1B_{1u}$) transition occurs at about 15 300 cm^{−1} (1.90 eV) that gives these dimeric compounds the observed dark blue-purple color. Finally, the diamagnetic-like behavior of the π -[TCNE]₂^{2−} dimers is due to population of only the singlet state for this coupled dimer.

Received: December 28, 2000

Revised: March 27, 2001 [Z16342]

- [1] "...there is a chemical bond between two atoms or groups of atoms in the case that the forces acting between them are such as to lead to an aggregate with sufficient stability to make it convenient for the chemist to consider it as an independent molecular species." L. Pauling, *The Nature of the Chemical Bond*, 3rd ed., Cornell University Press, Ithaca, 1960, p. 6.
- [2] G. Kaupp, J. Boy, *Angew. Chem.* **1997**, 109, 48; *Angew. Chem. Int. Ed. Engl.* **1997**, 36, 48; F. Toda, *Eur. J. Org. Chem.* **2000**, 1377.
- [3] C. Vazquez, J. C. Calabrese, D. A. Dixon, J. S. Miller, *J. Org. Chem.* **1993**, 58, 65.
- [4] See for example: A. H. Reis, Jr., E. Gebert, J. S. Miller, *Inorg. Chem.* **1981**, 20, 313; S. Z. Goldberg, B. Spivack, G. Stanley, R. Eisenberg, D. M. Braitsch, J. S. Miller, M. Abkowitz, *J. Am. Chem. Soc.* **1977**, 99, 110; M. C. Grossel, F. A. Evans, J. A. Hriljac, K. Prout, S. C. Weston, *J. Chem. Soc. Chem. Commun.* **1990**, 1494; M. T. Axcondo, L. Ballester, S. Golhen, A. Gutierrez, L. Ouahab, S. Yartsev, P. Delhaes, *J. Mater. Chem.* **1999**, 9, 1237; R. C. Hynes, J. R. Morton, K. F. Preston, A. J. Williams, F. Evans, M. C. Grossel, L. H. Sutcliffe, S. C. Weston, *J. Chem. Soc. Faraday Trans.* **1991**, 87, 2229; J. S. Miller, J. H. Zhang, W. M. Reiff, L. D. Preston, A. H. Reis, Jr., E. Gerbert, M. Extine, J. Troup, M. D. Ward, *J. Phys. Chem.* **1987**, 91, 4344.
- [5] M. T. Johnson, A. M. Arif, J. S. Miller, *Eur. J. Inorg. Chem.* **2000**, 1781, and references therein.

- [6] See for example: G. Zanotti, *Acta Crystallogr. Sect. B* **1982**, 38, 1225; J. S. Miller, P. J. Krusic, D. A. Dixon, W. M. Reiff, J. H. Zhang, E. C. Anderson, A. J. Epstein, *J. Am. Chem. Soc.* **1986**, 108, 4459; J. J. Mayerle, J. B. Torrance, *Bull. Chem. Soc. Jpn.* **1981**, 54, 3170; Y.-K. Yan, M. P. Mingos, T. E. Müller, D. J. Williams, *J. Chem. Soc. Dalton Trans.* **1995**, 2509; A. Marzotto, D. A. Clemente, L. Pasimeni, *J. Crystallogr. Spectrosc. Res.* **1988**, 18, 545.
- [7] *Handbook of Conducting Polymers* (Eds.: T. A. Skotheim, R. L. Elsenbaumer, J. R. Reynolds), 2nd ed., Marcel Dekker, New York, **1998**; J. R. Ferraro, J. M. Williams, *Introduction to Synthetic Electrical Conductors*, Academic Press, Orlando, **1987**.
- [8] J. M. Williams, *Organic Superconductors (Including Fullerenes): Synthesis, Structure, Properties, and Theory*, Prentice Hall, Englewood Cliffs, **1992**; T. Ishiguro, K. Yamaji, G. Saito, *Organic Superconductors*, Springer, New York, **1998**.
- [9] V. I. Ovcharenko, R. Z. Sagdeev, *Russ. Chem. Rev.* **1999**, 68, 345; M. Kinoshita, *Phil. Trans. R. Soc. London A* **1999**, 357, 2855; J. S. Miller, A. J. Epstein, *Chem. Commun.* **1998**, 1319; J. S. Miller, A. J. Epstein, *Chem. Eng. News* **1995**, 73(40), 30; J. S. Miller, A. J. Epstein, *Angew. Chem.* **1994**, 106, 399; *Angew. Chem. Int. Ed. Engl.* **1994**, 33, 385; O. Kahn, *Adv. Inorg. Chem.* **1995**, 43, 179.
- [10] See for example: J. S. Miller, J. C. Calabrese, H. Rommelmann, S. Chittipeddi, A. J. Epstein, J. H. Zhang, W. M. Reiff, *J. Am. Chem. Soc.* **1987**, 109, 769.
- [11] J. Zhang, L. M. Liable-Sands, A. L. Rheingold, R. E. Del Sesto, D. C. Gordon, B. M. Burkhardt, J. S. Miller, *Chem. Commun.* **1998**, 1385.
- [12] M. M. Olmsted, G. Speier, L. Szabo, *J. Chem. Soc. Chem. Commun.* **1994**, 541.
- [13] J. S. Miller, D. M. O'Hare, A. Charkraborty, A. J. Epstein, *J. Am. Chem. Soc.* **1989**, 111, 7853.
- [14] D. A. Lemervoskii, R. A. Stukan, B. N. Tarasevich, Tu. L. Slovokhotov, M. Yu. Antipin, A. E. Kalinin, Yu. T. Struchov, *Coord. Khim.* **1981**, 7, 118.
- [15] H. Bock, K. Ruppert, D. Fenske, H. Goesmann, *Z. Anorg. Allg. Chem.* **1995**, 595, 275.
- [16] J. S. Miller, J. C. Calabrese, C. Vazquez, R. S. McLean, D. T. Glatzhofer, J. W. Raebiger, *Inorg. Chem.* **2001**, 40, 2578.
- [17] S. A. Clemente, A. Marzotto, *J. Mater. Chem.* **1996**, 6, 941.
- [18] M. T. Johnson, C. F. Campana, B. M. Foxman, W. Desmarais, M. J. Vela, J. S. Miller, *Eur. J. Chem.* **2000**, 6, 1805.
- [19] J. R. Fox, B. M. Foxman, D. Guerrer, J. S. Miller, A. H. Reis, Jr., *J. Mater. Chem.* **1996**, 6, 1627.
- [20] Similar π -[TCNQ]₂^{2−} dimers have also been reported; see for example: H. Zhao, R. A. Heinz, K. R. Dunbar, R. D. Rogers, *J. Am. Chem. Soc.* **1996**, 118, 12844.
- [21] [TCNE]₂^{2−} dimers were selected due to the relative simplicity of the acceptor compared to other π -[A]₂^{2−} dimers.
- [22] All the computations were done using the Gaussian98 suite of programs. Gaussian 98 (Revision A.7), M. J. Frisch, G. W. Trucks, H. B. Schlegel, G. E. Scuseria, M. A. Robb, J. R. Cheeseman, V. G. Zakrzewski, J. A. Montgomery, R. E. Stratmann, J. C. Burant, S. Dapprich, J. M. Millam, A. D. Daniels, K. N. Kudin, M. C. Strain, O. Farkas, J. Tomasi, V. Barone, M. Cossi, R. Cammi, B. Mennucci, C. Pomelli, C. Adamo, S. Clifford, J. Ochterski, G. A. Petersson, P. Y. Ayala, Q. Cui, K. Morokuma, D. K. Malick, A. D. Rabuck, K. Raghavachari, J. B. Foresman, J. Cioslowski, J. V. Ortiz, B. B. Stefanov, G. Liu, A. Liashenko, P. Piskorz, I. Komaromi, R. Gomperts, R. L. Martin, D. J. Fox, T. Keith, M. A. Al-Laham, C. Y. Peng, A. Nanayakkara, C. Gonzalez, M. Challacombe, P. M. W. Gill, B. G. Johnson, W. Chen, M. W. Wong, J. L. Andres, M. Head-Gordon, E. S. Replogle, J. A. Pople, Gaussian, Inc., Pittsburgh, PA, **1998**.
- [23] First we explored this surface with RHF and RB3LYP calculations using the 6-31 + G and 6-31 + G(d) basis sets, which include diffuse functions for the proper description of the additional valence electron of the anion. All geometrical parameters except *r* were optimized for each point of this curve.
- [24] The minimum-energy structures were verified by looking at the number of nonimaginary frequencies. In all of the optimized geometries the frequencies were positive. Therefore, well-characterized minimum-energy structures of the π -[TCNE]₂^{2−} dimers were identified.

- [25] The presence of minima in a potential energy surface requires a transition state connecting these minima; this was observed for the π -[TCNE]₂²⁻ dimer (Figure 2). It originates from the energy required to reduce the bond order of the central C–C bond enabling the change in hybridization of the central C atom from sp² in conformer **3** to sp³ in conformer **2**. Near this maximum is the true transition state that separates **3** and **2**. More elaborate UB3LYP and MCSCF calculations—the UB3LYP calculations for the open-shell singlet (S₁) state were done within the broken symmetry approximation; the results of the broken symmetry calculations were tested by MCSCF(6,4) calculations on the potential energy curves of the π -[TCNE]₂²⁻ dimer, using a complete active space of six electrons and four orbitals; for these calculations the 6-31 + G basis set employed in the B3LYP calculations was used; for any given geometry, the population of the *b*_{2u}, *b*_{1g}, and antibonding *b*_{2u} orbitals in these MCSCF calculations differs by <0.1 e⁻ with respect to the B3LYP results for the same geometry, in agreement with the UB3LYP results; the shape of the S₀ and S₁ curves at the MCSCF level is also similar to that found at the UB3LYP level, and a full geometry optimization at the MCSCF level starting from the RB3LYP minimum goes towards dissociation into the fragments without a barrier—were run for each point in Figure 2, which confirmed the repulsive nature of the [TCNE]⁻⋯[TCNE]⁻ interaction, and also indicated that the π -[TCNE]₂²⁻ dimer **3** presents no barrier towards dissociation into two [TCNE]⁻ monomers, being the only minimum at short distances (the π -[TCNE]₂²⁻ dimer has *r* = 1.61 Å and average dihedral angles that range from 36.5 to 45.9°, and has *E*_{int} = 94.9 kcal mol⁻¹; see Supporting Information). Thus, the minimum nature of the π dimer in the RHF and RB3LYP calculations is an artifact of the double occupancy restriction imposed to the orbitals in these methods.
- [26] π -[TCNQ]₂²⁻ has been observed in solution: M. Itoh, *Bull. Chem. Soc. Jpn.* **1972**, 45, 1947; Y. Oohashi, T. Sakat, *Bull. Chem. Soc. Jpn.* **1973**, 46, 3330.
- [27] Preliminary calculations indicate that the size or type of the cation does not play an important role in the electrostatic stabilization.
- [28] This number is the result of adding $E(K_1^+ \cdots K_2^+) + E([TCNE]^- \cdots [TCNE]^-) + 2E([TCNE]^- \cdots K_1^+) + 2E([TCNE]^- \cdots K_2^+)$, which are, respectively, 30.5, 103.0, -70.9, and -75.0 kcal mol⁻¹; there are two different K⁺ ions in the K₂[TCNE]₂ aggregate, placed in a nonsymmetrical form relative to the [TCNE]⁻ ions (at 3.06 and 2.82 Å); this is the reason for the multiplication by two of the [TCNE]⁻⋯K⁺ interaction energy terms.
- [29] D. Braga, F. Grepioni, J. J. Novoa, *Chem. Commun.* **1998**, 1959; J. J. Novoa, I. Nobeli, F. Grepioni, D. Braga, *New J. Chem.* **2000**, 5; J. J. Novoa in *Implications of Molecular Materials Structure for New Technologies* (Eds.: J. A. K. Howard, F. H. Allen, G. P. Shields), Kluwer, Amsterdam, **1999**.
- [30] The nonlocal B3LYP exchange and correlation DFT functional and the 6-31 + G(2d,2p) basis set with a determinant in which the orbitals are not restricted to be doubly occupied were used. The B3LYP is a combination of the nonlocal three-parameter exchange functional (A. D. Becke, *J. Chem. Phys.* **1993**, 98, 5648) and the nonlocal LYP correlation functional (C. Lee, W. Yang, R. G. Parr, *Phys. Rev. B* **1998**, 37, 785).
- [31] a) P. Becker, P. Coppens, R. K. Ross, *J. Am. Chem. Soc.* **1973**, 95, 7604; b) D. A. Dixon, J. S. Miller, *J. Am. Chem. Soc.* **1987**, 109, 3656.
- [32] A. Zheludev, A. Grand, E. Ressouche, J. Schweizer, B. Morin, A. J. Epstein, D. A. Dixon, J. S. Miller, *J. Am. Chem. Soc.* **1994**, 116, 7243.
- [33] The tendency to delocalize the charge on the peripheral atoms cannot be attributed to the electronegativity of the CN group, as it is not found for either [C₂H₄]^{•-} or [C₂F₄]^{•-} by UB3LYP/6-31 + G(2d,2p) calculations, although F is more electronegative than the CN group. Therefore, this behavior can only be explained as associated delocalization due to the presence of low-energy resonance forms in which the unpaired electron is delocalized over the CN groups.
- [34] An “atoms-in-molecules” critical point analysis (R. F. Bader, *Atoms in Molecules*, Clarendon, Oxford, **1990**) on K₂[TCNE]₂ identifies the intradimer bonding as having (3, -1) bond critical points between the two [TCNE]⁻ units at the RB3LYP level.
- [35] J. B. Foresman, M. Head-Gordon, J. A. Pople, M. J. Frisch, *J. Phys. Chem.* **1992**, 96, 135.
- [36] There are also two weak peaks (ca. 10% of the intensity of the stronger peaks) at about 2200 cm⁻¹.
- [37] Similar results were noted for π -[TCNQ]₂²⁻: M. J. Rice, N. O. Lipari, S. Strassler, *Phys. Rev. Lett.* **1977**, 39, 1359.
- [38] It should be noted that in addition to the short C–C π bonding interactions, longer [TCNE]⁻⋯[TCNE]⁻ interactions are frequently present, but at these long distances (>3.5 Å) the bonding properties disappear, due to the exponential behavior of the orbital overlap integrals, responsible for Δ .